Design of an efficient mid-IR light source using chalcogenide holey fibers: a numerical study

2013 J. Opt. 15 035205

(http://iopscience.iop.org/2040-8986/15/3/035205)

IOP Publishing Journal of Optics
J. Opt. **15** (2013) 035205 (7pp) doi:10.1088/2040-8978/15/3/035205

Design of an efficient mid-IR light source using chalcogenide holey fibers: a numerical study

A Barh[1], S Ghosh[1], G P Agrawal[2], R K Varshney[1], I D Aggarwal[3] and B P Pal[1]

[1] Physics Department, Indian Institute of Technology Delhi, Hauz Khas, New Delhi 110016, India
[2] Institute of Optics, University of Rochester, Rochester, NY 14627, USA
[3] Physics Department, University of North Carolina, Charlotte, NC 28223, USA

E-mail: bppal@physics.iitd.ernet.in

Received 15 October 2012, accepted for publication 25 January 2013
Published 26 February 2013
Online at stacks.iop.org/JOpt/15/035205

Abstract
We report the design of a highly nonlinear holey fiber for making a mid-infrared light source at 4.36 μm. A solid-core chalcogenide-based index-guided holey microstructured optical fiber with circular air holes has been exploited to numerically demonstrate wavelength translation via four-wave mixing. We employ a thulium-doped fiber laser as the pump with a power of 5 W. Our simulations indicate that a maximum parametric gain of 20.5 dB with a bandwidth of 16 nm is achievable in this designed fiber, resulting in a power conversion efficiency of more than 17.6%.

Keywords: nonlinear optics, four-wave mixing, microstructured fibers

(Some figures may appear in colour only in the online journal)

1. Introduction

In recent years a strong interest has emerged in developing devices capable of operating at wavelengths in the mid-IR range (2–25 μm) in view of their potential applications in areas as wide as astronomy, climatology, civil, medical surgery, military, biological spectroscopy, optical frequency metrology, optical tomography and sensing [1–5]. To design fiber-based devices for these mid-IR applications, chalcogenide glasses (S–Se–Te-based glass compositions) are promising candidates because of their extraordinary linear and nonlinear intrinsic properties [6–8]. However, realization of low transmission losses in chalcogenide microstructured optical fibers (MOFs) is still a challenging issue [9]. As the constituent atoms are relatively heavy, the vibrational energies of chalcogenide glasses are low, which results in a very good transparency in the mid-infrared region and, as a consequence, their low phonon energies make them attractive as hosts for rare-earth dopants [10]. On the other hand, their chemical durability, glass transition temperature, strength, stability etc can be improved by doping with As, Ge, Sb or Ga for drawing an optical fiber. At present their fabrication technology is well matured though expensive [5, 9, 11, 12].

Since chalcogenide glasses exhibit a relatively high Kerr nonlinearity (achievable n_2 being as high as 100 times larger than that of conventional silica fiber) [13] these glasses can enable signal processing [9], all optical switching [13], supercontinuum generation, wavelength conversion from the available near IR sources to the targeted mid- to long-IR range, etc [14]. Apart from chalcogenide, silicon photonics based mid-IR wavelength translation has also been demonstrated [15]. Additionally, studies on chalcogenide MOFs have shown that the zero-dispersion wavelengths in such fibers can be made to fall anywhere within a very broad infrared wavelength range (2–11 μm) through appropriate fiber designs. Moreover, other attractive features such as endlessly single-mode behavior [16], wide tunability of mode effective area (A_{eff}) [17], etc make MOFs a suitable platform to exploit for realizing fiber-based light sources in the mid-IR wavelengths through the technique of wavelength translation

via four-wave mixing (FWM). In this paper, our aim is to numerically design an arsenic sulfide (As_2S_3)-based MOF light source within the wavelength range of 4–5 μm using a commercially available continuous-wave (CW) thulium (Tm)-doped fiber laser as a pump for the FWM process.

2. Numerical model

We focus on an As_2S_3-based MOF geometry with a solid core and holey cladding. Amongst various chalcogenide glasses, the reported transmission loss in As_2S_3 fibers is sufficiently low (~0.2 dB m in a 500 m-long fiber) in our targeted wavelength regime [11]. In optical fibers, several nonlinear phenomena could be exploited to generate new wavelength(s) [6]. Under certain conditions, however, FWM is the dominant nonlinear mechanism for generating new wavelengths, provided a certain phase-matching condition is satisfied [6, 18]. For our intended design, we will be dealing with average input pump powers (P_0) below 5 W, which is considerably lower than the threshold for the onset of stimulated Raman and Brillouin scatterings in fibers shorter than 10 m [6]. Our aim is to carry out a feasibility design of an As_2S_3-based solid-core MOF light source in the wavelength range 4–5 μm with a commercially available CW Tm-doped fiber laser as the pump through single-pump FWM.

As is well known [6], during the FWM process, two pump photons of frequency ω_p get converted into a signal photon ($\omega_s < \omega_p$) and an idler photon ($\omega_i > \omega_p$) according to the energy conservation relation ($2\omega_p = \omega_s + \omega_i$), where subscripts s, i and p stand for signal, idler, and pump, respectively. For efficient FWM, the phase-matching condition is very important, and the fiber's dispersion profile should be so designed such that its zero-dispersion wavelength (λ_{ZD}) falls close to the pump wavelength.

Assuming quasi-CW conditions for all the three waves, the complex amplitudes $A_j(z)$ ($j = p, i, s$) inside the fiber satisfy the following three coupled equations [6, 19]:

$$\frac{dA_p}{dz} = -\frac{\alpha_p A_p}{2} + \frac{in_2\omega_p}{c}\left[\left(f_{pp}|A_p|^2 + 2\sum_{k=i,s} f_{pk}|A_k|^2\right) \times A_p + 2f_{ppis}A_p^* A_i A_s e^{j\Delta\kappa z}\right] \quad (1)$$

$$\frac{dA_i}{dz} = -\frac{\alpha_i A_i}{2} + \frac{in_2\omega_i}{c}\left[\left(f_{ii}|A_i|^2 + 2\sum_{k=p,s} f_{ik}|A_k|^2\right) \times A_i + f_{ispp}A_s^* A_p^2 e^{-j\Delta\kappa z}\right] \quad (2)$$

$$\frac{dA_s}{dz} = -\frac{\alpha_s A_s}{2} + \frac{in_2\omega_s}{c}\left[\left(f_{ss}|A_s|^2 + 2\sum_{k=p,i} f_{sk}|A_k|^2\right) \times A_s + f_{sipp}A_i^* A_p^2 e^{-j\Delta\kappa z}\right] \quad (3)$$

where α_j is the loss at the wavelength λ_j, n_2 is the nonlinear index coefficient and $\Delta\kappa$ is the effective phase mismatch, defined as [6]

$$\Delta\kappa = \sum_{m=2,4,6\ldots}^{\infty} 2\beta_m(\omega_p)\frac{\Omega_S^m}{m!} + \Delta k_W. \quad (4)$$

In this expression for $\Delta\kappa$, the first term is due to the effects of material, whereas the second term represents the waveguide contribution. The values β_m are the mth order group velocity-dispersion (GVD) parameter. Ω_s is the frequency shift ($\Omega_s = \omega_p - \omega_s = \omega_i - \omega_p$). We can neglect Δk_W for single-mode fibers [6]. The overlap integrals are defined as

$$f_{jk} = \frac{\langle|F_j|^2|F_k|^2\rangle}{\langle|F_j|^2\rangle\langle|F_k|^2\rangle} \quad (5)$$

$$f_{ijkl} = \frac{\langle F_i^* F_j^* F_k F_l\rangle}{[\langle|F_i|^2\rangle\langle|F_j|^2\rangle\langle|F_k z|^2\rangle\langle|F_l|^2\rangle]^{1/2}} \quad (6)$$

where $F_j(x, y)$ is the spatial distribution of the fiber mode for the jth field. Here, we have assumed that spatial modes experience more or less uniform n_2 (n_2 of As_2S_3 material), as the maximum fraction of A_{eff}, which overlaps with the air hole region, is only 0.1. To achieve the maximum frequency shift through the FWM process, $\Delta\kappa$ should ideally be zero. Thus considering up to fourth-order dispersion terms, the best route to achieve the phase-matching criterion for FWM would be to tailor the total dispersion through fiber design so as to bring the zero-dispersion wavelength (λ_{ZD}) very close to the pump wavelength (λ_p) while maintaining a small positive value for β_2 and a large negative value for β_4. We also need to maintain the cutoff wavelength for the first higher order mode as low as possible (below λ_p); for this to occur, the hole diameter to pitch ratio (d/Λ) of the MOF should be low (<0.45). However, during the numerical optimization process we also realized that it is very difficult to simultaneously achieve a positive β_2 and a large negative β_4 for this range of d/Λ; an increase in d/Λ is needed. Additionally, to enhance the nonlinearity and to minimize the confinement loss (α_c), A_{eff} should be as low as possible at both λ_p and λ_s.

3. Proposed design

In our design calculations, we have balanced all the above-mentioned criteria by choosing an optimized set of fiber parameters and by introducing a different size for air holes in the second cladding ring (radius of air holes in this ring is denoted as r_2) (see figure 1) embedded within the As_2S_3 matrix. Here, r is the radius of air holes in the remaining rings in the holey cladding. All simulations were carried out by considering a MOF with five rings of air holes as constituting the cladding. Dispersion parameters as well as the modal field were calculated using the commercially available CUDOS® software in conjunction with MATLAB® for other numerical calculations. To calculate dispersion characteristics of the chosen MOF geometry, the wavelength dependence of the linear refractive index [n (λ)] of the As_2S_3 glass has been incorporated through the Sellmeier formula [20]. We used $n_2 = 4.2 \times 10^{-18}$ m^2 W^{-1} at the pump wavelength [14]. We chose a CW Tm-doped fiber laser emitting at 2.04 μm

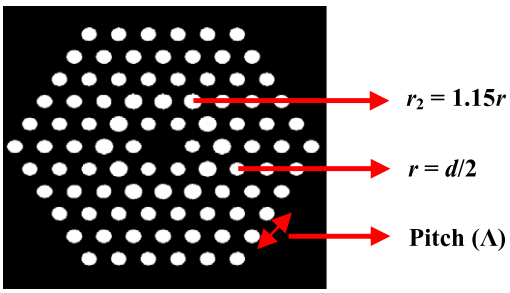

Figure 1. Cross sectional view of the designed MOF. Cladding consists of five rings of air holes (white circles) embedded in the As_2S_3 matrix (black background). The radius of the air holes in the second cladding ring is r_2, whereas the center-to-center air hole separation is denoted as pitch (Λ).

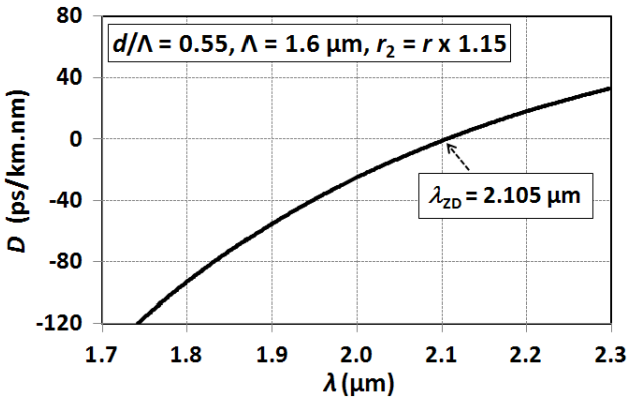

Figure 3. Calculated total dispersion of the designed MOF.

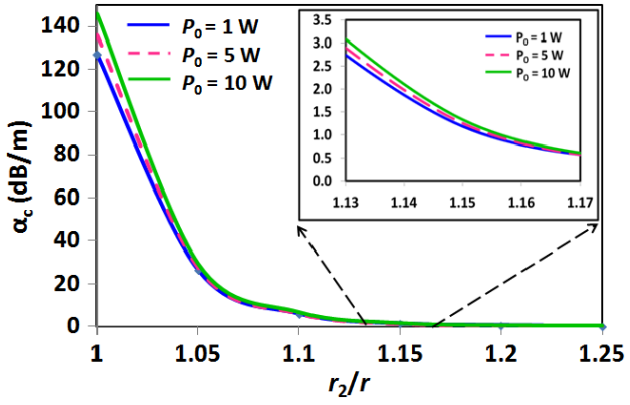

Figure 2. Variation of α_c with r_2/r for three different P_0, a larger view of the proposed design is shown in the inset.

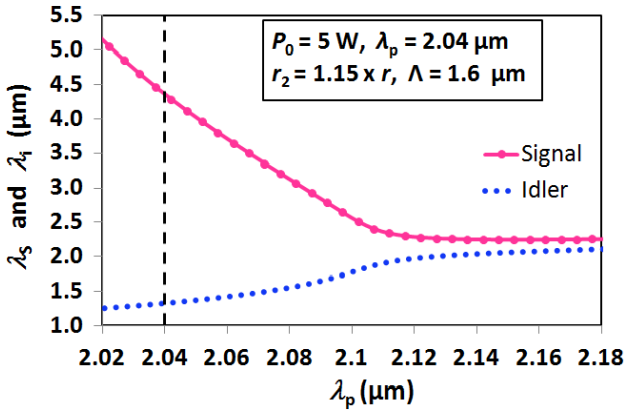

Figure 4. FWM phase-matching curve for the designed MOF. The vertical dashed line indicates the used pump position.

as the required pump. During optimization of the MOF structure, a strong interplay was evident between Ω_s, parametric amplification, and α_c with variations in r_2. After optimization, a high amplification with a considerably low α_c ($\sim$1.2 dB m^{-1}) at the generated signal wavelength (λ_s) of 4.36 μm was theoretically achieved for $d/\Lambda = 0.55$, $\Lambda = 1.6$ μm and for $r_2 = 1.15r$. The α_c variation with r_2/r is shown in figure 2 for different values of P_0.

The dispersion versus wavelength is shown in figure 3, where it is evident that the achieved λ_{ZD} at 2.105 μm is very close to but greater than λ_p, which is the primary requirement for our design. The values of β_2 and β_4 are respectively 32.68 ps^2 km^{-1} and -1.62×10^{-3} ps^4 km^{-1} near this λ_p.

4. Wavelength translation through the proposed nonlinear fiber design

The generated signal wavelength as a function of pump wavelength is shown in figure 4 for an assumed pump power of 5 W. We can see that as λ_p shifts away from λ_{ZD} (still in the normal dispersion regime) the signal is generated at a higher wavelength and the idler occurs at a lower wavelength. But, simultaneously, the FWM efficiency will decrease as the pump–signal, pump–idler and signal–idler overlap integrals become smaller. We define the quantity amplification factor (AF$_j$) as P_j/P_{in} for $j = $ i, s and P_j/P_0 for $j = $ p. Here P_j is the output power at length L and P_{in} is the input idler power. The launch of a weak idler along with the pump improves the FWM efficiency since stimulated FWM is employed in place of spontaneous FWM. Note that here we are using the idler as an input field and call the new wavelength generated in the mid-IR region the signal.

As the material loss is very high around the idler wavelength, the AF$_i$ automatically gets reduced. While solving the three coupled equations, we have taken the material loss to be 50 dB m^{-1} for $\lambda < 1.4$ μm [21] and for higher wavelengths we take the material loss as reported in [14]. Assuming a pump at 2.04 μm, the signal is generated at 4.36 μm for an idler launched at 1.33 μm.

After optimizing, we fixed this input idler power (P_{in}) at 8 mW. For $P_{in} = 8$ mW and $P_0 = 5$ W, we have studied variations of the amplitudes, output powers (P_{out}) and AF along the fiber length (L) for the designed MOF. These are shown in figures 5(a)–(c), respectively. From figure 5, we can interpret that, unlike the signal, the high loss at λ_i reduces its P_{out} and AF at larger lengths. Thus idler power almost dies out after a meter length of the designed fiber. But the signal power decreases quite slowly along L. We optimized the length of this MOF by choosing AF$_s$ > 20 dB, which yielded the required fiber length as 1.36 m for this P_{in} value (8 mW).

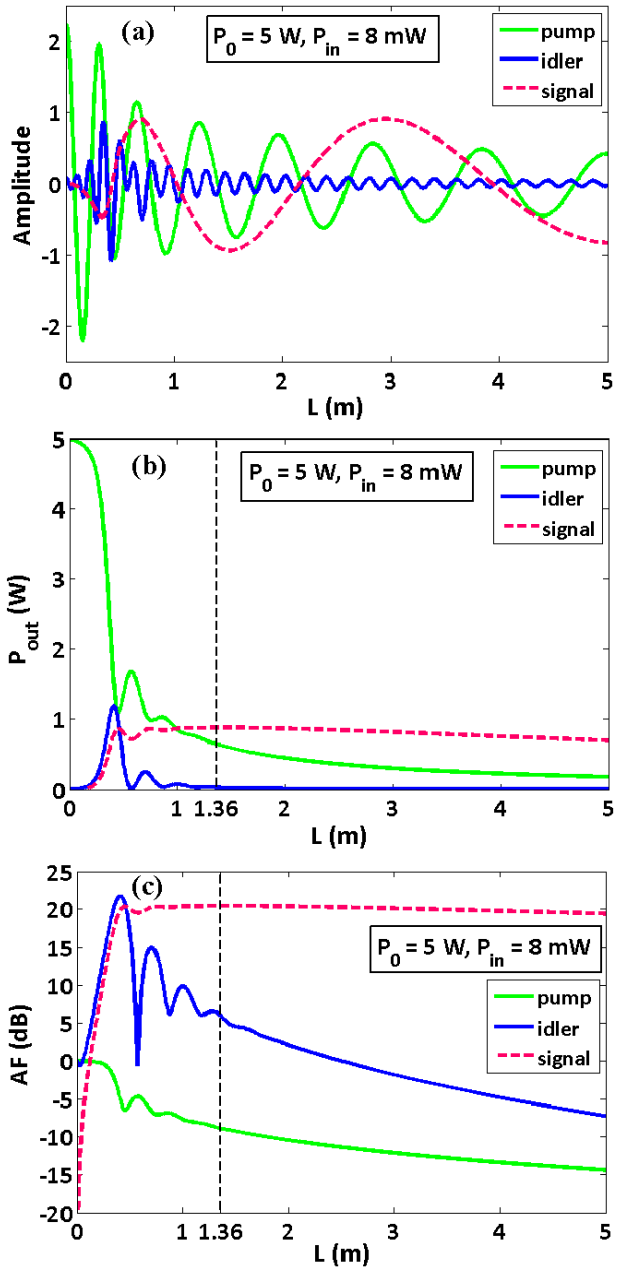

Figure 5. Variation of (a) amplitude (in $W^{1/2}$), (b) output power and (c) amplification factor of the pump, signal and idler along the fiber length (L). The vertical dashed line indicates the optimum length for which $AF_s \sim 20$ dB (it is the maximum value of AF_s for $P_{in} = 8$ mW).

After a fiber length of 1.36 m, the achieved signal power (P_s) is 0.88 W, which corresponds to a FWM power conversion efficiency (P_s/P_0) of 17.6%. Note that here we have used the same n_2 value for both λ_p and λ_s. However for more accurate modeling, inclusion of a wavelength dependent n_2 is desirable. Lack of availability of a universally valid $n_2(\lambda)$ for longer wavelengths ($\lambda > 3$ μm) is a problem. Nevertheless, to get an indicative estimate for $n_2(\lambda)$, we obtained through extrapolation from [14, 22] its value as $\approx 2 \times 10^{-18}$ m^2 W^{-1} at $\lambda = 4.36$ μm. As this estimation may not necessarily be accurate, as an indicator for the potential influence of $n_2(\lambda)$

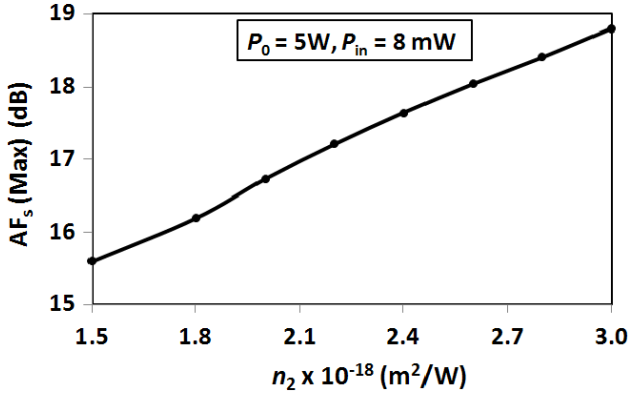

Figure 6. Maximum AF_s variation with nonlinear index coefficient (n_2) at the signal wavelength.

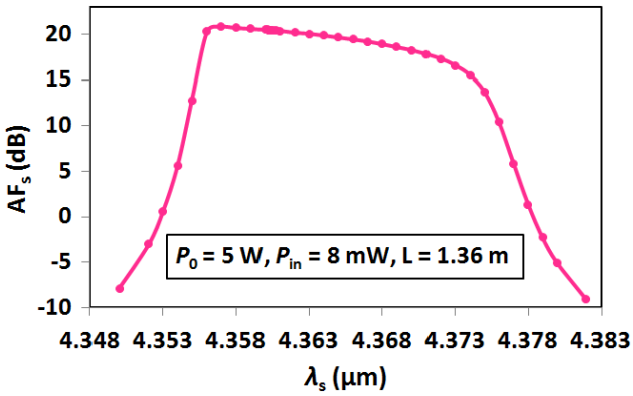

Figure 7. AF_s variation of the generated signal ($\lambda_s = 4.36$ μm) for $\lambda_p = 2.04$ μm and $P_0 = 5$ W. The 3 dB band width is $\sim$16 nm.

on AF_s, the variation of the optimized AF_s with n_2 ranging from 1.5×10^{-18} m^2 W^{-1} to 3×10^{-18} m^2 W^{-1} is studied and shown in figure 6, in which it can be seen that AF_s correspondingly varies from 15.6 to 18.8 dB.

To find the band width (BW) of the generated signal, we studied the AF_s around the generated λ_s. Despite very high AF_s ($\sim$20.5 dB) the spectrum shown in figure 7 is quite narrow (3 dB BW $\sim$16 nm). We may mention that by tuning P_0, we can change P_s as well as AF_s, e.g. for a pump power of 10 W, P_s becomes 1.784 W.

5. Tolerance study

From the potential fabrication point of view, we have also studied the tolerance of the structure to variations in the MOF's geometrical parameters (r_2, r, and Λ). Here, only the AF_s, P_s, λ_s and λ_i variations are shown.

5.1. Effect of variation in r_2

Even a variation in r_2 of as much as $\pm$10% has very little effect on the value of the signal wavelength, its AF_s, and P_s, as shown in figures 8(a)–(c), respectively.

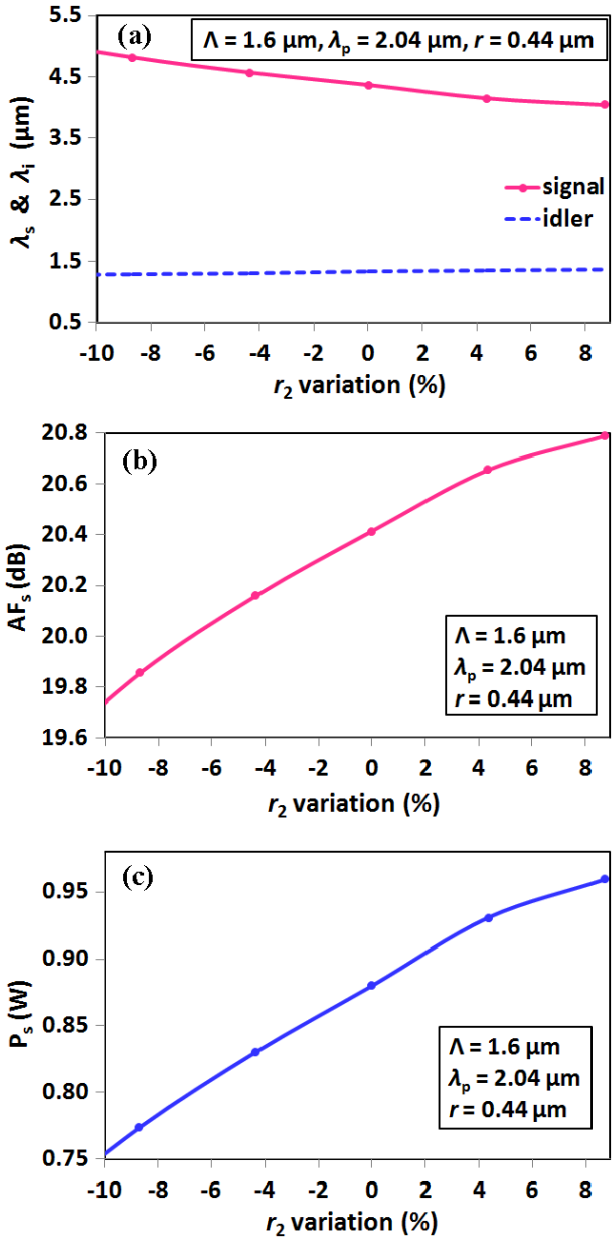

Figure 8. Dependence of (a) generated signal and idler wavelengths, (b) signal amplification factor, and (c) output signal power on varying r_2 for fixed values of Λ and r.

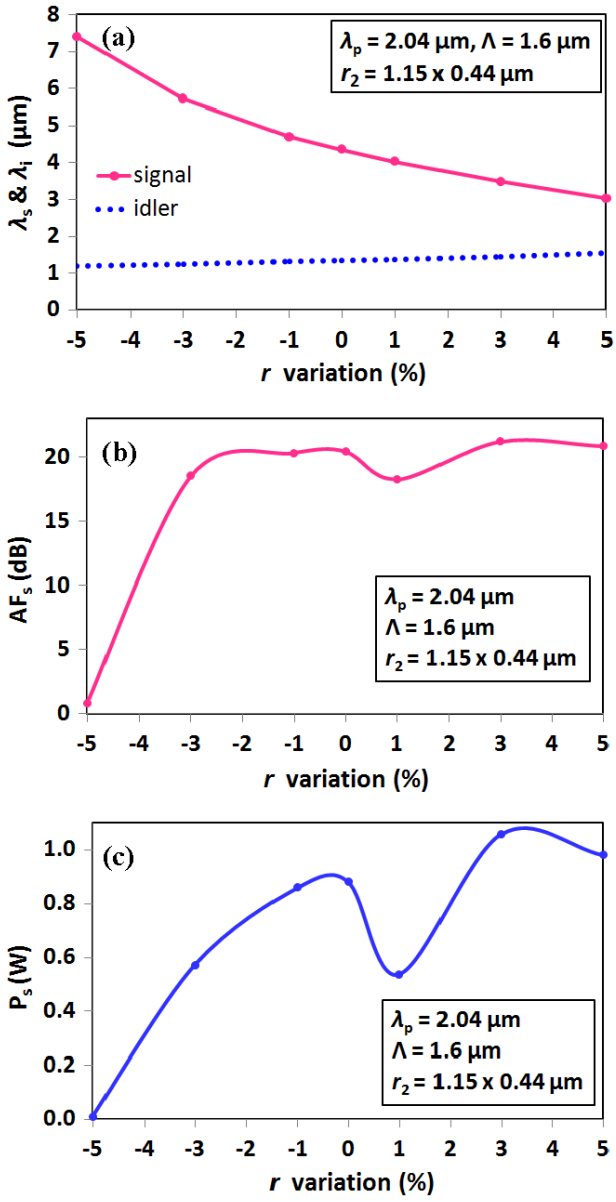

Figure 9. Dependence of (a) generated λ_s and λ_i, (b) signal amplification factor, and (c) output signal power on varying r for fixed values of Λ and r_2.

The figures revealed that AF_s remains almost flat around 20.5 dB for the above-mentioned variations in fiber parameters around our proposed design. AF_s is >19 dB and P_s is >0.75 W for variations in r_2 up to $\pm 10\%$. Thus r_2 is not a very critical parameter from the fabrication point of view for the designed MOF. However, we should mention that the choice of r_2 could significantly influence the confinement loss at λ_s (cf figure 2). This fact can be appreciated from figure 2, which shows that the confinement loss is quite high ($\approx$120 dB m^{-1}) for $r_2 = r$ but around our proposed design parameter ($r_2/r = 1.15$) the loss is significantly lower (1.2 dB m^{-1}) and it is almost independent of variations in the pump power.

5.2. *Effect of variation in r*

By varying r by $\pm 5\%$, the effect on λ_s, λ_i, AF_s and P_s were studied and shown in figures 9(a)–(c), respectively. From figure 9(a) we can see that the effect of variation in r is quite strong on the values of λ_s and λ_i.

For lower r values, as λ_{ZD} shifts away from λ_p, the λ_s and λ_i get further separated, which results in a decrease of the overlap integrals (f). Thus, the AF_s and power fall rapidly on decreasing r by -3%. On the other hand, as r increases, both λ_s and λ_i move nearer to the pump wavelength (2.04 μm). Thus, both material loss (α) and f become favorable for efficient FWM (α decreases and f increases). However, AF_s and P_s still drop for higher r. This may be attributed to the increase in FWM performance for larger values of r, as the

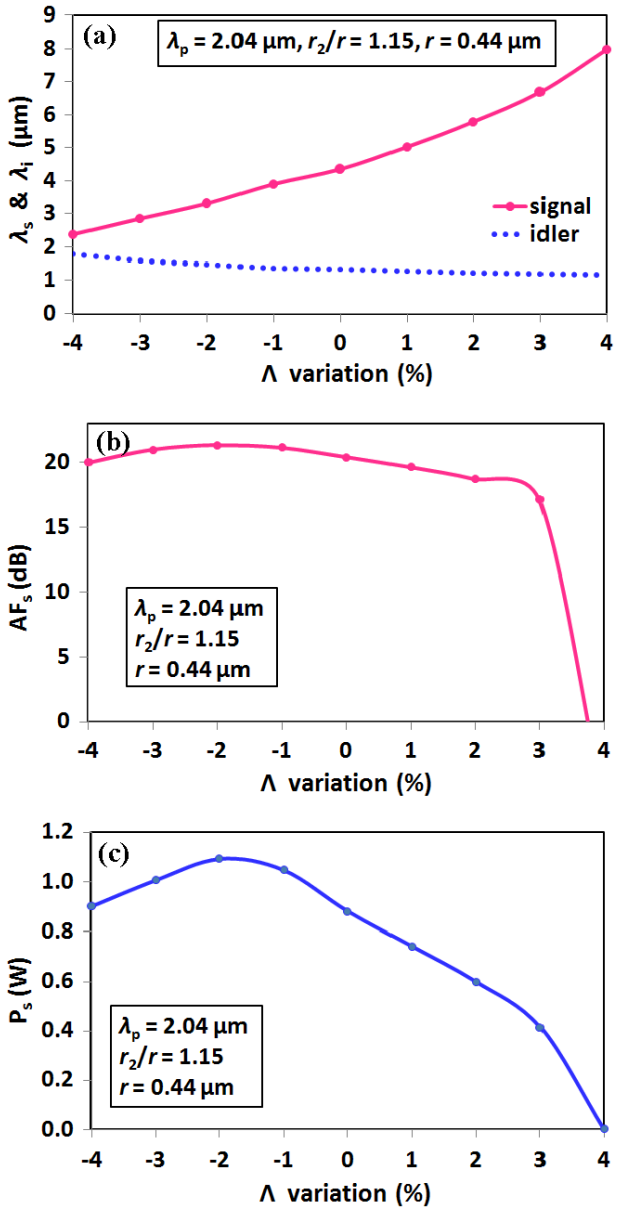

Figure 10. Variation of (a) generated λ_s and λ_i, (b) signal amplification factor, and (c) output signal power due to a variation in Λ for fixed values of r and the ratio r_2/r.

maximum power coupling from pump to signal and idler wavelengths occurs for shorter fiber length. Here, we have performed all of our calculations for a fixed L of 1.36 m, which is optimum for $r = 0.44$ μm. As a result, an increase in r also results in a decrease in the AF_s and P_s for $L = 1.36$ m.

The dip in AF_s and P_s for a variation in r by $+1\%$ is due to a comparatively large material loss at a wavelength of 4 μm in As_2S_3 (H–S bond absorption) [14].

5.3. Effect of variation in Λ

Variations in $\lambda_s, \lambda_i, AF_s$ and P_s were studied (shown in figures 10(a)–(c), respectively) on varying the pitch Λ by $\pm 4\%$.

With an increase in Λ , λ_{ZD}, λ_s and λ_i shift away from λ_p. The conclusions made above for a variation in r can be drawn for this case also. All of these studies were carried out by considering a discrete value of Λ. So, unlike r variation, no signal is generated at 4 μm in this case. That is why the AF_s and P_s curves look smoother (no dip) around our proposed design.

The effect of a variation in Λ is a little more critical than a variation in r, as we can see from figures 9(b), (c) and 10(b), (c) that AF_s is >18 dB and P_s is >0.5 W for a variation in Λ of -4% to $+3\%$ and for a variation in r of -4% to $+5\%$.

For efficient signal output we also need to maintain the output idler power (P_i) as low as possible. Our study reveals that P_i can be maintained below 50 mW for an r_2 variation of up to $\pm 10\%$, an r variation of -4% to $+2\%$ and a Λ variation of up to $\pm 2\%$.

According to [23], the fabrication tolerance for Λ and the diameter of the holes (d) with respect to their average value can be achieved within 2%–4%. Our numerical studies revealed that the maximum limit of tolerable imperfections lie well within this fabrication tolerance limit. Moreover, with the state-of-the-art techniques, since all the holes are not distorted in the same way in practice, some averaging effect in hole sizes is likely to occur. Such a fiber, if experimentally realized, should be attractive as a mid-IR light source for the variety of applications mentioned in the introduction.

6. Conclusions

Through a detailed numerical study, for the first time to the best of our knowledge, we have shown that mid-IR power levels in excess of 1 W are achievable by using a 2.04 μm fiber laser as the pump with moderate power levels of 6–7 W. Additionally, a relatively narrow bandwidth (16 nm), a high conversion efficiency (>17%), and a very low confinement loss (1.2 dB m^{-1}) at the generated signal wavelength of 4.36 μm (λ_s) should make our proposal attractive for making an all-fiber mid-IR light source. Potential application areas could be mid-IR spectroscopy, astronomy and defense, since the generated wavelength matches the second low-loss transparency window of the terrestrial atmosphere.

It should be interesting to explore specialty fiber designs along similar lines to realize tunable mid-IR sources through the use of a tunable pump. It would be interesting to undertake fabrication of chalcogenide fibers based on this design, and if required through further fine tuning of the fiber parameters, though there could be several fabrication challenges. For example, accuracy in maintaining the required r_2, r, Λ values throughout the fiber length, preparation of pure, low-loss, stable, stoichiometric As_2S_3 glasses, minimization of end-face reflections etc have to be investigated experimentally. However, the very fact that there already exist well-matured fabrication technologies [11, 12, 24] for chalcogenide MOF means it should be of interest to invest efforts and money in the fabrication of the proposed fiber design in view of its potential use in the civil as well as defense sectors. Perhaps CVD, MCVD [5], molding processes [25] or casting techniques [26] will be

good options for the fabrication of these specialty fibers and our methodology should serve as the initial design for the experimental realization of such a mid-IR fiber light source.

Acknowledgments

This work relates to Department of the Navy (USA) Grant N62909-10-1-7141 issued by Office of Naval Research Global. The United States Government has a royalty-free license throughout the world in all copyrightable material contained herein. The authors acknowledge useful comments offered by Jash Sanghera of NRL (Washington) on the manuscript.

AB gratefully acknowledges the award of a Senior PhD fellowship by CSIR (India).

References

[1] Sanghera J S and Aggarwal I D 1999 *J. Non-Cryst. Solids* **6** 256–7
[2] Rolfe P 2000 *Annu. Rev. Biomed. Eng.* **2** 715–54
[3] Serebryakov V A, Boĭko É V, Petrishchev N N and Yan A V 2010 *J. Opt. Technol.* **77** 6–17
[4] Hartl I, Li X D, Chudoba C, Ghanta R K, Ko T H, Fujimoto J G, Ranka J K and Windeler R S 2001 *Opt. Lett.* **26** 608–10
[5] Hewak D W 2011 *Nature Photon.* **5** 474
[6] Agrawal G P 2007 *Nonlinear Fiber Optics* 4th edn (San Diego, CA: Academic)
[7] Zakery A and Elliott S R 2003 *J. Non-Cryst. Solids* **330** 1–12
[8] Boudebs G, Cherukulappurath S, Guignard M, Troles J, Smektala F and Sanchez F 2004 *Opt. Commun.* **230** 331–6
[9] Eggleton B J, Luther-Davies B and Richardson K 2011 *Nature Photon.* **5** 141–8
[10] Tver'yanovich Y S and Tverjanovich A 2004 *Semicond. Semimetals* **80** 169–207
[11] Sanghera J S, Aggarwal I D, Shaw L B, Busse L E, Thielen P, Nguyen V, Pureza P, Bayya S and Kung F 2001 *J. Optoelectron. Adv. Mater.* **3** 627–40
[12] El-Amraoui M *et al* 2010 *Opt. Express* **18** 26655–65
[13] Harbold J M, Ilday F O, Wise F W, Sanghera J S, Nguyen V Q, Shaw L B and Aggarwal I D 2002 *Opt. Lett.* **27** 119–21
[14] Hu J, Menyuk C R, Shaw L B, Sanghera J S and Aggarwal I D 2010 *Opt. Lett.* **35** 2907–9
[15] Liu X, Kuyken B, Roelkens G, Baets R, Osgood R M Jr and Green W M J 2012 *Nature Photon.* **6** 667–71
[16] Birks T A, Knight J C and Russell P St J 1997 *Opt. Lett.* **22** 961–3
[17] Mortensen N A 2002 *Opt. Express* **10** 341–8
[18] Lin C, Reed W A, Pearson A D and Shang H T 1981 *Opt. Lett.* **6** 493–5
[19] Cappellini G and Trillo S 1991 *J. Opt. Soc. Am.* B **8** 824–38
[20] Chaudhari C, Suzuki T and Ohishi Y 2009 *J. Light. Technol.* **27** 2095–9
[21] Viens J F, Meneghini C, Villeneuve A, Galstian T V, Knystautas E J, Duguay M A, Richardson K A and Cardinal T 1999 *J. Light. Technol.* **17** 1184–91
[22] Weiblen R J, Docherty A, Hu J and Menyuk C R 2010 *Opt. Express* **18** 26666–74
[23] Poletti F, Finazzi V, Monro T M, Broderick N G R, Tse V and Richardson D J 2005 *Opt. Express* **13** 3728–36
[24] Sanghera J S, Florea C, Busse L, Shaw B, Miklos F and Aggarwal I D 2010 *Opt. Express* **18** 26760–8
[25] Quentin C *et al* 2010 *Proc. SPIE* **7598** 75980
[26] Coulombier Q *et al* 2010 *Opt. Express* **18** 9107–12